

# Transcriptome analysis revealed growth phase-associated changes of a centenarian-originated probiotic *Bifidobacterium animalis* subsp. *lactis* A6

Hui Wang

China Agricultural University

Jieran An

China Agricultural University

Chengfei Fan

China Agricultural University

Zhengyuan Zhai

China Agricultural University

Hongxing Zhang

Beijing University of Agriculture

Yanling Hao (✉ [haoyl@cau.edu.cn](mailto:haoyl@cau.edu.cn))

China Agricultural University

---

## Research Article

**Keywords:** Bifidobacterium animlis subsp. lactis A6, RNA-seq, growth phase, Tad pili, adhesion

**Posted Date:** November 12th, 2021

**DOI:** <https://doi.org/10.21203/rs.3.rs-1036916/v1>

**License:** © ⓘ This work is licensed under a Creative Commons Attribution 4.0 International License.

[Read Full License](#)

---

**Version of Record:** A version of this preprint was published at BMC Microbiology on February 25th, 2022.  
See the published version at <https://doi.org/10.1186/s12866-022-02474-5>.

# Abstract

## Background

The physiology and application characteristics of probiotics are closely associated with the growth phase. *Bifidobacterium animalis* subsp. *lactis* A6 is a promising probiotic strain isolated from the feces of a healthy centenarian in China. In this study, RNA-seq was carried out to investigate the metabolic mechanism between the exponential and the stationary phase in *B. lactis* A6.

## Results

Differential expression analysis showed that a total of 810 genes were significantly changed in the stationary phase compared to the exponential phase, which consisted of 392 up-regulated and 418 down-regulated genes. The results showed that the transport and metabolism of cellobiose, xylooligosaccharides and raffinose were enhanced at the stationary phase, which expanded carbon source utilizing profile to confront with glucose consumption. Meanwhile, genes involved in  $\text{NH}_3$  production were up-regulated at the stationary phase to enhance acid tolerance during fermentation. In addition, peptidoglycan biosynthesis was significantly repressed, which is comparable with the decreased growth rate during the stationary phase. Remarkably, a putative gene cluster encoding Tad pili was up-regulated 6.5~12.1-fold, which is consistent with the significantly increased adhesion rate to mucin from 2.38–4.90% during the transition from the exponential phase to the stationary phase.

## Conclusions

This study reported growth phase-associated changes of *B. lactis* A6 during fermentation, including expanded carbon source utilizing profile, enhanced acid tolerance, and up-regulated Tad pili gene cluster responsible for bacterial adhesion in the stationary phase. These findings provide a novel insight into the growth phase associated characteristics in *B. lactis* A6 and provide valuable information for further application in the food industry.

## Background

Probiotics are defined as “live microorganisms which when administered in adequate amounts confer a health benefit on the host” [1]. Some probiotics confer a number of health-promoting benefits to human host, such as competitive exclusion of pathogenic bacteria, modulation of immune system and enhancement of epithelial barrier function [2–4]. Therefore, probiotics, mainly including lactobacilli and bifidobacterial, have been widely applied as food and dietary supplements [5]. However, the physiology and application characteristics of probiotics are closely associated with the growth phase. After spray drying, the viability of *L. rhamnosus* GG was approximately 20 times higher at stationary phase than that of cells from the exponential phase [6]. Meanwhile, the maximum adhesion ability of *L. rhamnosus* GG to

Caco-2 cells at the early stationary phase was ten times higher than that of cells at the exponential phase [7]. Therefore, some research was widely performed to reveal the metabolic mechanism underlying the different growth of probiotics in recent years.

Transcriptomic analysis revealed a shift from the cell division gene expression at the lag phase to a carbohydrate metabolism-related gene repertoire at the exponential growth phase in *Bifidobacterium bifidum* PRL2010 [8]. Meanwhile, transcriptomic analysis of *L. casei* Zhang showed that genes involved in carbohydrate metabolism, inorganic ion transport, and chaperones were highly expressed at the stationary phase, whereas genes related to nucleotide transport and metabolism, energy production and conversion were predominantly expressed during the exponential phase [9]. Furthermore, combined transcriptomic and proteomic analyses demonstrated that the shift from glucose fermentation to galactose utilization and the transition from homolactic to mixed acid fermentation were observed from the exponential to the stationary growth phase [10].

*Bifidobacterium animalis* subsp. *lactis* A6 (*B. lactis* A6) was isolated from a healthy centenarian in the Bama County of the Guangxi Zhuang Autonomous Region in China, which is famous for having a population with a high life-expectancy. Previous study showed that *B. lactis* A6 had high acid resistance to low pH and could improve obesity in mice [11, 12]. In addition, as the Next-Generation Sequencing technology, RNA-Seq provides higher efficiency and sensitivity compared with microarray methods [13]. In this study, RNA-seq was performed to investigate the growth phase-related changes between the exponential and stationary phase in *B. lactis* A6. Our results will provide new insights for the rational application of *B. lactis* A6 as probiotics.

## Results

### Growth of *B. lactis* A6 strain in MRSc broth

In order to investigate the change of growth situation, *B. lactis* A6 was cultured in 15 ml MRSc broth for 24 h. The OD<sub>600</sub> was 0.2 and 3.4 at the beginning of the exponential and stationary phase, respectively, and the pH was reduced to 4.6 at 24 h (**Fig. 1**). In this study, samples were collected at the exponential phase with OD<sub>600</sub> 0.6~0.8 and the stationary phase with OD<sub>600</sub> 4.0~4.2 for transcriptome analysis to determine growth phase-associated changes in *B. lactis* A6.

### Global gene expression profiles in the stationary phase compared to the exponential phase

The number of clean reads and the information of reads mapping to the reference genome are shown in **Table S1** and **S2**. After removing low quality reads and adaptor sequences, more than 19.6 million high-quality reads per sample were generated. The clean reads were aligned to the whole reference genome sequence, and more than 99% of the clean reads for each sample were mapped to the genome. Correlation of gene expression level between independent biological replicates was shown by the Pearson's correlation coefficient, which was more than 0.872 for each sample (**Fig. S1**). These results indicated the obtained transcriptome data were suitable for further analysis. Differential expression

analysis showed that a total of 810 DEGs consisted of 392 up-regulated and 418 down-regulated genes in the stationary phase (A6\_WD) compared to the exponential phase (A6\_log) (Adjusted *P* value < 0.05, **Fig. 2A**). The putative functions of these genes were classified in different categories grouped by the gene ontology (GO) (**Fig. 2B** and **Fig. S2**). The DEGs involved in various biological processes, such as carbohydrate uptake and metabolism, oligopeptides uptake and peptidoglycan biosynthesis, acid tolerance resistance and bacterial adhesion to mucin will be discussed in detail as follows.

### Carbon source utilization profile was expanded during the stationary phase

In this study, *BAA6\_1092* encoding a putative glucose uptake permease was down-regulated 5.4-fold during the stationary phase. Meanwhile, 18 genes involved in glucose metabolism called “the bifid shunt” were also down-regulated 1.6~4.1-fold during the stationary phase (**Table S3** and **Fig. 3B**). Among them, gene *BAA6\_0968* encoding fructose-6-phosphate/xylulose-5-phosphate phosphoketolase was decreased 2.0-fold, which catalyzes the conversion of xylulose 5-phosphate or fructose 6-phosphate to acetyl phosphate [14]. Furthermore, *ldh2*, *pfl*, and *ackA* encoding lactate dehydrogenase, formate acetyltransferase and acetate kinase were down-regulated 3.1, 4.1 and 1.7-fold, respectively, which are involved in the production of L-lactate, formate and acetate.

However, genes *BAA6\_0517-0518* and *BAA6\_1585-1587* encoding two ABC-type transporters for uptake of XOS and raffinose were up-regulated 1.9~3.4-fold during the stationary phase. Meanwhile, genes *BAA6\_0481* and *BAA6\_0050* encoding two putative MFS transporters for the uptake of GOS and gentiobiose were up-regulated 5.2 and 3.2-fold, respectively (**Table S3** and **Fig. 3A**). Moreover, gene *BAA6\_1415* encoding a putative cellobiose ABC transporter permease protein CebG and *BAA6\_1416* encoding cellobiose phosphorylase CbpA were increased 3.4 and 5.6-fold, respectively. Exogenous cellobiose is transported into the bacterial cell by CebG, then catalyzed by CbpA to yield one molecular of glucose-1-phosphate and glucose [15]. Remarkably, the transcriptional level of gene *araA*, *araB*, and *araD* for L-arabinose metabolism to xylulose-5-P and gene *xylB* for xylulose metabolism were all up-regulated over 2.0-fold at the stationary phase (**Table S3** and **Fig. 3B**). These results indicated that *B. lactis* A6 attenuates the glycolysis pathway in response to glucose consumption during fermentation, but expands its carbon source utilization profile to L-arabinose, xylose, and cellobiose for survival.

### Oligopeptides uptake was enhanced to adapt to changes in growth

In this study, genes involved in Met, Asp, Tyr, Phe, Arg, Pro and Gln biosynthesis were repressed during the stationary phase (**Table S3**). Meanwhile, three pairs of genes encoding ABC-type amino acid transport systems for Asp, Glu and Met were found down-regulated 1.8~4.0-fold. However, the *opp* operon (*BAA6\_0566-0570*) encoding an ABC oligopeptide transporter oppABCDF was upregulated 2.0~5.3-fold, which are involved in the uptake of di- and tripeptides [16]. Meanwhile, gene *dppD* and *dppC* encoding DppD and DppC components of DppABCDF complex were increased 5.7 and 4.6-fold, respectively. DppABCDF is specialized in dipeptide transportation to support bacterial growth in *Escherichia coli* [17]. Remarkably, genes *BAA6\_0186* and *BAA6\_0230* encoding two dipeptidases were all up-regulated over 1.6-fold. Dipeptidase catalyzes the hydrolysis of dipeptides to produce free amino acids for bacterial

growth [18]. Therefore, *B. lactis* A6 tends to utilize exogenous amino acids by oligopeptides uptake, rather than *de novo* synthesis of single amino acid during the stationary phase, which elaborates a potential survival strategy for bacteria to adapt to environmental changes during growth.

### Peptidoglycan biosynthesis were repressed in the stationary phase

In this study, gene *BAA6\_0562* encoding glutamine-fructose-6-phosphate transaminase was down-regulated 2.0-fold during the stationary phase, which catalyzes the formation of glucosamine-6-phosphate (GlcN-6P) from fructose-6P (**Fig. S3**). GlcN-6P was subsequently catalyzed by phosphoglucosamine mutase encoded by *BAA6\_1325* to form GlcN-1P. The Gene *glmU* encoding a bifunctional protein GlmU was also down-regulated 3.0-fold, which catalyzes the biosynthesis of UDP-N-acetylglucosamine from GlcN-1P [19]. Additionally, *murC*, *murD*, and *murF* were down-regulated over 1.50-fold, which are involved in the addition of L-alanine, D-glutamate, and D-alanyl-D-alanine to UDP-N-acetylmuramate to form the skeletal structure of a DAP-type peptidoglycan. Moreover, gene *BAA6\_0083* encoding transpeptidase (DD-TPase) and *murJ* encoding a putative peptidoglycan lipid II flippase were also down-regulated 1.7 and 1.6-fold, respectively. DD-TPase was reported to synthesize cross-linked peptidoglycan from lipid intermediates, and then the lipid-linked peptidoglycan precursors were transported from the inner cytoplasmic membrane to the outer leaflet by flippase during cell wall formation [20, 21]. Furthermore, gene *BAA6\_0084* encoding a bacterial cell division membrane protein and genes *BAA6\_0550*, *BAA6\_1198*, and *BAA6\_1201* encoding cell division protein FtsX, FtsQ, and FtsW were all down-regulated around 2.0~3.4-fold during the stationary phase (**Table S3**). Taken all together, genes involved in peptidoglycan biosynthesis, a key cell wall component in bifidobacteria, and cell division were generally repressed during the stationary phase in *B. lactis* A6, reflecting a retarded growth situation at this stage.

### Acid tolerance response

Gene *serB* encoding phosphoserine phosphatase for the biosynthesis of serine was up-regulated 1.8-fold. Meanwhile, gene *BAA6\_0572* encoding cystathionine beta-synthase (CysK) and *BAA6\_0947* encoding cystathionine beta-lyase (MetC) were upregulated 2.7 and 6.3-fold during the stationary phase, respectively. (**Table S3**). CysK catalyzes the synthesis of cystathionine from homocysteine and serine, and MetC catalyzes the cleavage of cystathionine to homocysteine, pyruvate and  $\text{NH}_3$ , which constitute the cysteine and cystathionine cycle in response to acid stress [22]. Moreover, gene *BAA6\_0010* encoding a NADP-specific glutamate dehydrogenase was upregulated 2.7-fold, which catalyzes glutamate to 2-oxoglutarate and  $\text{NH}_3$ . In contrast, gene *BAA6\_0708* and *BAA6\_1220* encoding glutamine synthetase 1 and 2 were respectively down-regulated 6.2- and 1.9-fold, which are involved in catalyzing the biosynthesis of glutamine from glutamate and  $\text{NH}_3$ . Therefore, the net production of  $\text{NH}_3$  was increased during the stationary phase.

In addition, gene *livK* encoding a substrate-binding protein for the transport of branched-chain amino acids (BCAAs) was up-regulated 3.1-fold at the stationary phase. Meanwhile, *BAA6\_0283* encoding

acetolactate synthase and *BAA6\_0146* encoding ketol-acid reductoisomerase were also up-regulated 2.3- and 3.2-fold, respectively. Acetolactate synthase catalyzes the biosynthesis of acetolactate and 2-aceto-2-hydroxybutanoate from pyruvate, which are further catalyzed by ketol-acid reductoisomerase for Val and Leu biosynthesis or for Ile production [23]. The transport and biosynthesis of BCAAs were enhanced during the stationary phase compared to the exponential phase. Remarkably, molecular chaperone GroEL/ES complex encoded by *BAA6\_0370* and *BAA6\_0665*, and DnaK encoded by *BAA6\_1543* were all upregulated over 1.2-fold during the stationary phase. Meanwhile, *BAA6\_0675* encoding ATP-binding subunit ClpE and *BAA6\_1072~1073* encoding two Clp protease proteolytic subunits ClpP1 and ClpP2 were also upregulated 1.7, 1.6 and 3.2-fold, respectively (**Table S3**). These results showed that *B. lactis* A6 delivered multiple strategies to respond acid stress with lactic acid production during fermentation.

### Adhere ability to mucin was enhanced during the stationary phase

In this study, a putative gene cluster of *BAA6\_0205~0212* involved in type IVb (Tad) pili biosynthesis was obviously up-regulated 6.5~12.1-fold during the stationary phase compared to the log phase (**Table S3**). Among them, genes *flp*, *tadE* and *tadF* encoding a fimbrial protein prepilin and two pseudopilins were upregulated 7.5, 8.6 and 8.1-fold, respectively, which are participated in prepilin proteins biosynthesis. Meanwhile, gene *tadV* encoding a prepilin peptidase was up-regulated 1.6-fold in the stationary phases. Prepilin peptidase catalyzes the formation of mature pilin from prepilin proteins [24]. In addition, *tadZ* and *tadABC* encoding four Fli pilus assembly proteins involved in pilus assembly and localization were also up-regulated 9.4, 6.5, 12.1 and 9.5-fold, respectively.

Furthermore, the amino acid sequence alignment of Tad pili between *B. breve* UCC2003 and *B. lactis* A6 was performed with SnapGene software (from Insightful Science, version 5.3) in a local alignment (Smith-Waterman) model. The results showed an amino acid sequence identity among 34.2%-59.3% (**Table S4** and **Fig. 4**). Tad pili is an important adhesive structure identified in bifidobacteria [25], and the adhesion of *B. lactis* A6 to mucin showed that the adhesion rate was 4.90% with bacterial cells at the stationary phase, significantly higher than that of 2.38% with bacterial cells at the exponential phase (**Fig. 5**). These findings further confirmed the adhesion to mucin was expressed in a growth phase-dependent manner in *B. lactis* A6 strain, and the enhanced expression of Tad pili may facilitate its colonization and maintenance in the intestine of host receptor.

## Discussion

Probiotics are widely accepted to be beneficial for the maintenance of the gut homeostasis, improvement of the immune system, and amelioration of various metabolic disease [26, 27]. In recent years, the consumption of probiotics to promote health has grown rapidly worldwide and become an independent industry [28]. Notably, the physiology and application characteristics of probiotics are closely associated with the growth phase. Many studies have focused on the overall growth phase-associated changes during fermentation based on transcriptome and/or proteome technology [9, 10, 29]. In this study, RNA-seq was carried out to investigate the metabolic mechanism between the exponential and the stationary

phase in *B. lactis* A6. The glycolysis pathway was obviously slowed down during the stationary phase with glucose consumption, which is shown by most of down-regulated genes involved in the bifid shunt. However, a typical characteristic was observed for the potential transport and utilization of cellobiose by CebG and CbpA. *B. lactis* A6 was isolated from the feces of a Bama centenarian, whose diet was rich in plant-based fibers [30]. Plant derived carbohydrates, such as cellulose, was catalyzed to produce soluble cellobiose by cellobiohydrolases in the human gut [31]. Therefore, the up-regulation of cellobiose transport and utilization could contribute to the adaptation of *B. lactis* A6 in the intestine of healthy centenarians.

For acid tolerance response, *B. lactis* A6 exhibited various strategies to regulate the pH reduction during growth, including enhanced  $\text{NH}_3$  and BCAAs production and up-regulated expression of molecular chaperone and Clp protease. In bacteria,  $\text{NH}_3$  could neutralize cytoplasmic  $\text{H}^+$  to enhance the acid tolerance [32]. The synthesis of BCAAs like Leu, Val, and Ile were reported for building proteins with high hydrophobicity [33], which contributes to protect proteins against attack of bile by building hydrophobic areas in *B. longum* subsp. *longum* BBMN68 [18]. In addition, the up-regulation of BCAAs biosynthesis and a shifting to BCAA metabolism for energy production were also reported in the acid tolerance response of *B. longum* subsp. *longum* BBMN68 [22]. Thus, the enhanced branched-chain amino acids transport and biosynthesis may contribute to against acid stress in *B. lactis* A6 during the stationary phase. Furthermore, molecular chaperone and Clp protease have been reported for participating general stress responses. GroEL/ES complex could prevent misfolding of proteins and promote the refolding and proper assembly of unfolded polypeptides under stress conditions [34]. Dnak, belonging to an Hsp70 protein, can actively unfold misfolded structures, leading to gradual disaggregation of aggregated polypeptides [35]. Clp proteases could recognizes and degrades irreversibly damaged proteins in response to acid stress [22]. The upregulated Clp proteases for degradation of damaged proteins could facilitate amino acids recycling in *B. lactis* A6 under acid stress.

Colonization in the mammalian gastrointestinal tract by microbes is believed to play an essential part to confer health benefits [36]. A Tad pili encoding gene cluster - "*tad*<sub>2003</sub>" locus was identified in *B. breve* UCC2003, which was proved to be essential for colonization and persistence in murine gut as a conserved host-colonization factor [37]. The "*tad*<sub>2003</sub>" locus encodes eight proteins for the biosynthesis of a mature Tad pilus. TadE and TadF are participated in the prepilin precursor biosynthesis, and TadA is an ATPase to provide energy for Fli-pilus assembly. TadB and TadC are thought to channel the energy of ATP hydrolysis into Fli-pilus polymerization or serve as an inner membrane scaffold for the assembly of the pilus biogenesis apparatus. Then the Tad apparatus is directed to the cell poles by TadZ [24, 38]. In this study, a putative Tad pili encoding gene cluster *BAA6\_0205 ~ 0212* was highly expressed during the stationary phase, which exhibited similar gene cluster structure and higher amino acid identity of 34.2%-59.3% with "*tad*<sub>2003</sub>" locus. In addition, Tad pili could bind to carbohydrate moieties present in glycoproteins or glycolipids receptors of mucus layer, which covered on the surface of intestinal epithelial cells [39, 40]. Thus, the enhanced expression of Tad pili in *B. lactis* A6 strain during the stationary phase may facilitate its colonization and maintenance in the intestine of the host. To verify the hypothesis, the

adhesion rate of *B. lactis* A6 to mucin *in vitro* was performed under the log and stationary phase, respectively. The results showed that the adhesion rate to mucin was approx. 2-fold increased with stationary phase bacterial cells than that with exponential phase cells.

## Conclusions

Probiotic bacteria harvested at different phases of growth has been shown to cause the different application characteristics and mucosal responses in human [6, 7]. Accordingly, growth phase-associated changes of *B. lactis* A6 was investigated by RNA-Seq in MRSc broth. In this study, *B. lactis* A6 expanded the carbon source utilizing profile to transport cellobiose, XOS and raffinose to confront with glucose consumption in the stationary phase. In addition, *B. lactis* A6 was isolated from the feces of a Bama centenarian, whose diet was rich in plant-based fibers [30]. Therefore, the up-regulation of cellobiose, XOS and raffinose transport and utilization could contribute to the adaptation of *B. lactis* A6 in the intestine of healthy centenarians. Meanwhile, this bacterium developed the acid stress strategies during fermentation, including the enhanced  $\text{NH}_3$  production. Remarkably, a putative gene cluster encoding Tad pili was significantly up-regulated at the stationary phase, which was correspondingly enhance bacterial adhesion to mucin at this stage. These findings provide a novel insight into the growth phase associated characteristics in *B. lactis* A6 and provide valuable information for further application of *B. lactis* A6 in the food industry.

## Methods

### Bacterial strains and culture conditions

A -80°C glycerol stock of *B. lactis* A6 was anaerobically incubated at 37°C in de Man-Rogosa-Sharp broth supplemented with 0.05% (w/v) L-cysteine (MRSc) for 24 h, followed by 1% (v/v) inoculation to a 15 mL MRSc broth for overnight. The pH and optical density at 600 nm ( $\text{OD}_{600}$ ) were recorded at 2-h intervals.

### RNA extraction

Overnight culture of *B. lactis* A6 strain was inoculated (1% v/v) into a 15 mL fresh MRSc broth. Samples were collected at the exponential phase with  $\text{OD}_{600}$  0.6~0.8 and the stationary phase with  $\text{OD}_{600}$  4.0~4.2. Total RNA was extracted using TRIzol reagent (Invitrogen, Carlsbad, CA) and purified using the TURBO DNA-free Kit (Ambion, Austin, TX, USA) according to the manufacturer's instructions. RNA concentration was measured using Qubit® RNA Assay Kit in Qubit® 2.0 Fluorometer (Life Technologies, CA, USA). RNA integrity was assessed using the RNA Nano 6000 Assay Kit of the Agilent Bioanalyzer 2100 system (Agilent Technologies, CA, USA).

### RNA-seq

Sequencing libraries were generated using NEBNext® Ultra™ Directional RNA Library Prep Kit for Illumina® (NEB, USA). Index codes were added to attribute sequences to each sample. The library



fragments were purified with AMPure XP system (Beckman Coulter, Beverly, USA) to select cDNA fragments of 150~200 bp in length. Then 3 µl USER Enzyme (NEB, USA) was used with size-selected, adaptor-ligated cDNA at 37°C for 15 min followed by 95°C for 5 min. The PCR was performed using Phusion High-Fidelity DNA polymerase (NEB) with Universal PCR primers and Index (X) primer. Finally, PCR products were purified by AMPure XP system (Beckman Coulter) and the library quality was assessed on the Agilent Bioanalyzer 2100 system (Agilent Technologies). The library preparations were sequenced on an Illumina HiSeq platform and paired-end reads were generated.

### Transcriptomic data processing

Raw data of fastq format were firstly processed through in-house perl scripts. Clean reads were obtained by removing reads containing adapter, reads containing ploy-N or reads with low quality from raw data. All clean reads were aligned to the genome of *B. lactis* A6 with GenBank Accession No. NZ\_CP010433.1 by Bowtie2-2.2.3 [41]. HTSeq v0.6.1 was then used to count the reads numbers mapped to each gene [42]. Differential expression analysis of samples at the stationary growth phase relative to exponential phase was performed using the DESeq R package (V1.18.0) [43]. Genes with an adjusted *P*-value < 0.05 detected by DESeq were assigned as differentially expressed.

### Bacterial adhesion to mucin

The adherence of bacteria to mucin was performed as described by Xiong et al. [44]. Briefly, Nunc MaxiSorp 96-well microplate (Thermo Fisher Scientific, Denmark) was coated with 100 µL of mucin (from porcine stomach; Sigma-Aldrich, USA) and incubated for 16 h at 4°C at a concentration of 2.5 pmol per well. The wells were then washed twice with PBS and incubated with 2% (w/v) bovine serum albumin for 2 h at 37°C. The wells were subsequently washed three times with PBS. The bacteria collected at the exponential and stationary phase were washed twice with PBS and resuspended to a final OD<sub>600</sub> equivalent to  $\sim 2\text{--}3 \times 10^8$  CFU/mL. Then 200 µL of bacterial suspension were added to coated 96-well plates and incubated at 37°C for 1 h. The unattached bacteria were removed by washing the wells for 3 times with PBS, and then treated with 200 µL 0.05% (v/v) Triton X-100 and incubated at 37°C for 30 min. The adhesion ratios (%) were calculated by comparing the bacterial counts after adhesion to the number of cells originally added to the plate wells. The results were obtained by three independent experiments.

### Statistical analysis

Data were analyzed using GraphPad Prism 8 software for Windows (GraphPad Software, Inc., La Jolla, CA, USA). Results were presented as the mean value ± standard deviation. An unpaired Student t-test was used to calculate *P* values when two groups were compared.

## Abbreviations

*B. lactis* A6

*Bifidobacterium animalis* subsp. *lactis* A6

RNA-seq  
RNA-sequencing technology  
MRSc  
de Man-Rogosa-Sharp broth with L-cysteine  
DEGs  
differential expression genes  
GO  
gene ontology  
XOS  
xylooligosaccharides  
GOS  
galactooligosaccharides  
GlcN-6P  
glucosamine-6-phosphate  
GlcN-1P  
glucosamine-1-phosphate  
BCAAs  
branched-chain amino acids  
Tad pili  
type IVb pili

## **Declarations**

### **Acknowledgements**

This work was supported by the Key Laboratory of Functional Dairy, Co-constructed by Ministry of Education and Beijing Municipality, and College of Food Science and Nutritional Engineering, China Agricultural University, Beijing, China.

### **Funding**

This work was supported by the National Key Research and Development Program of China (2018YFC1604303).

### **Availability of data and materials**

All the raw data of transcriptome sequencing could be downloaded from GEO with the Accession No. GSE173957.

### **Author contributions**

YH and HZ designed the experiments; HW performed the experiments; HW and JA analyzed the data; CF contributed to the materials, and analysis tools; HW wrote the paper, YH and ZZ revised the final

manuscript. All authors read and approved the final manuscript.

### **Ethics approval and consent to participate**

Not applicable

### **Consent for publication**

Not applicable

### **Competing interests**

The authors declare no conflict of interest.

## **References**

1. Hill C, Guarner F, Reid G, Gibson GR, Merenstein DJ, Pot B, et al. The International Scientific Association for Probiotics and Prebiotics consensus statement on the scope and appropriate use of the term probiotic. *Nat. Rev. Gastroenterol Hepatol.* 2014;11(8):506-14.
2. Bron PA, Kleerebezem M, Brummer RJ, Cani PD, Mercenier A, Macdonald TT, et al. Can probiotics modulate human disease by impacting intestinal barrier function? *Br. J. Nutr.* 2017;117(01):93-107.
3. Mörk S, Butler MI, Holl A, Cyran JF, Dinan TG. Probiotics and the microbiota-gut-brain axis: focus on psychiatry. *Curr Nutr Rep.* 2020;9(8):171-82.
4. Sanders ME, Merenstein DJ, Reid G, Gibson GR, Rastall RA. Probiotics and prebiotics in intestinal health and disease: from biology to the clinic. *Nat. Rev. Gastroenterol. Hepatol.* 2019;16(Suppl. 1):605-16.
5. Rivera-Espinoza Y, Gallardo-Navarro Y. Non-dairy probiotic products. *Food Microbiol.* 2010;27(1):1-11.
6. Broeckx G, Kiekens S, Jokicevic K, Byl E, Henkens T, Vandenheuvel D, et al. Effects of initial cell concentration, growth phase, and process parameters on the viability of *Lactobacillus rhamnosus* GG after spray drying. *Dry. Technol.* 2020;38(11):1474-92.
7. Deepika G, Green RJ, Frazier RA, Charalampopoulos D. Effect of growth time on the surface and adhesion properties of *Lactobacillus rhamnosus* GG. *J. Appl. Microbiol.* 2009;107(4):1230-40.
8. Turroni F, Foroni E, Montanini B, Viappiani A, Strati F, Duranti S, et al. Global genome transcription profiling of *Bifidobacterium bifidum* PRL2010 under in vitro conditions and identification of reference genes for quantitative real-time PCR. *Appl. Environ. Microbiol.* 2011;77(24):8578-87.
9. Wang J, Zhang W, Zhi Z, Wei A, Bao Q, Yong Z, et al. Gene expression profile of probiotic *Lactobacillus casei* Zhang during the late stage of milk fermentation. *Food Control.* 2012;25(1):321-7.

10. Laakso K, Koskenniemi K, Koponen J, Kankainen M, Surakka A, Salusjärvi T, et al. Growth phase-associated changes in the proteome and transcriptome of *Lactobacillus rhamnosus* GG in industrial-type whey medium. *Microb. Biotechnol.* 2011;4(6):746-66.
11. Sun E, Zhao L, Ren F, Liu S, Zhang M, Guo HY. Complete genome sequence of *Bifidobacterium animalis* subsp. *lactis* A6, a probiotic strain with high acid resistance ability. *J. Biotechnol.* 2015;200:8-9.
12. Huo Y, Lu X, Wang X, Wang X, Chen L, Guo H, et al.. *Bifidobacterium animalis* subsp. *lactis* A6 alleviates obesity associated with promoting mitochondrial biogenesis and function of adipose tissue in mice. *Molecules.* 2020;25(7):1490.
13. Mäder U, Nicolas P, Richard H, Bessi res P, Aymerich S. Comprehensive identification and quantification of microbial transcriptomes by genome-wide unbiased methods. *Curr. Opin. Biotechnol.* 2011;22(1):32-41.
14. Glenn K, Smith KS. Allosteric regulation of *Lactobacillus plantarum* xylulose 5-phosphate/fructose 6-phosphate phosphoketolase (Xfp). *J. Bacteriol.* 2015;197(7):1157-63.
15. Yernool DA, McCarthy JK, Eveleigh DE, Bok JD. Cloning and characterization of the glucooligosaccharide catabolic pathway  $\beta$ -glucan glucohydrolase and cellobiose phosphorylase in the marine hyperthermophile *Thermotoga neapolitana*. *J. Bacteriol.* 2000;182:5172-9.
16. Higgins CF. ABC transporters: from microorganisms to man. *Annu. Rev. Cell Biol.* 1992;8(1):67-113.
17. Abouhamad WN, Manson M, Gibson MM, Higgins CF. Peptide transport and chemotaxis in *Escherichia coli* and *Salmonella typhimurium*: characterization of the dipeptide permease (Dpp) and the dipeptide-binding protein. *Mol Microbiol.* 2010;5(5):1035-47.
18. An H, Douillard FP, Wang G, Zhai Z, Yang J, Song S, et al. Integrated transcriptomic and proteomic analysis of the bile stress response in a centenarian-originated probiotic *Bifidobacterium longum* BBMN68. *Mol. Cell Proteomics.* 2014;13(10):2558-72.
19. Mengin-Lecreulx D, Heijenoort J. Copurification of glucosamine-1-phosphate acetyltransferase and N-acetylglucosamine-1-phosphate uridyltransferase activities of *Escherichia coli*: characterization of the glmU gene product as a bifunctional enzyme catalyzing two subsequent steps in the pathway for UDP-N-acetylglucosamine synthesis. *J. Bacteriol.* 1994;176(18):5788-95.
20. Sung MT, Lai YT, Huang CY, Chou LY, Shih HW, Cheng WC, et al. Crystal structure of the membrane-bound bifunctional transglycosylase PBP1b from *Escherichia coli*. *Proc. Natl. Acad. Sci. USA.* 2009;106(22):8824-9.
21. Sham LT, Butler EK, Lebar M, Kahne D, Bernhardt TG, Ruiz N. MurJ is the flippase of lipid-linked precursors for peptidoglycan biogenesis. *Science.* 2014;345(6193):220.

22. Jin J, Bing Z, Guo H, Cui J, Jiang L, Song S, et al. Mechanism analysis of acid tolerance response of *Bifidobacterium longum* subsp. *longum* BBMN 68 by gene expression profile using RNA-sequencing. PLoS One. 2012;7(12):e50777.
23. Huo Y, Zhan Y, Wang Q, Li S, Yang S, Nomura CT, et al. Acetolactate synthase (AlsS) in *Bacillus licheniformis* WX-02: enzymatic properties and efficient functions for acetoin/butanediol and L-valine biosynthesis. Bioproc Biosyst Eng. 2018;41(1):87-96.
24. Tomich M, Planet PJ, Figurshi DH. The tad locus: postcards from the widespread colonization island. Nat. Rev. Microbiol. 2007;5(5):363-75.
25. Grimm V, Westermann C, Riedel CU. Bifidobacteria-host interactions—an update on colonisation factors. Biomed Res Int. 2014;960826.
26. Zhao Y, Zeng Y, Zeng D, Wang HS, Zhou MJ, Sun N, et al. Probiotics and microRNA: their roles in the host-microbe interactions. Front Microbiol. 2021;604462.
27. Varsha KK, Maheshwari AP, Nampoothiri KM. Accomplishment of probiotics in human health pertaining to immunoregulation and disease control. Clin Nutr ESPEN. 2021;44:26-37.
28. Lu K, Dong SW, Wu XY, Jin RM, Chen HB. Probiotics in Cancer. Front Oncol. 2021;11:638148.
29. Mozzetti V, Grattepanche F, Moine D, Berger B, Rezzonico E, Arigoni F, et al. Transcriptome analysis and physiology of *Bifidobacterium longum* NCC2705 cells under continuous culture conditions. Benef Microbes. 2012;3(4):261-72.
30. Wang F, Yu T, Huang GH, Cai D, Liang XL, Sun HY, et al. Gut microbiota community and its assembly associated with age and diet in Chinese centenarians. J Microbiol Biotechnol. 2015;25(8):1195-1204.
31. Cantarel BL, Lombard V, Henrissat B. Complex carbohydrate utilization by the healthy human microbiome. PLoS One. 2012;7(6):e28742.
32. van de Guchte M, Serror P, Chervaux C, Smokvina T, Ehrlich SD, Maguin E. Stress responses in lactic acid bacteria. Anton Leeuw Int J G. 2002;82(1-4):187-216.
33. Sánchez B, Champomier-Vergès MC, Anglade P, Baraige F, Reyes-Gavilan CGD, Margolles A, et al. Proteomic analysis of global changes in protein expression during bile salt exposure of *Bifidobacterium longum* NCIMB 8809. J Bacteriol. 2005;187(16):5799-808.
34. Zhai Z, Yang Y, Wang H, Wang G, Ren F, Li Z, et al. Global transcriptomic analysis of *Lactobacillus plantarum* CAUH2 in response to hydrogen peroxide stress. Food Microbiol. 2020;87:103389.
35. Mayer MP, Bukau BJC, Sciences ML. Hsp70 chaperones: Cellular functions and molecular mechanism. Cell Mol Life Sci. 2005;62(6):670-84.

36. Shanahan F. The colonic microflora and probiotic therapy in health and disease. *Curr Opin Gastroen.* 2011;27(1):61-5.
37. Motherway MO, Zomer A, Leahy SC, Reunanen J, Bottacini F, Claesson MJ, et al. Functional genome analysis of *Bifidobacterium breve* UCC2003 reveals type IVb tight adherence (Tad) pili as an essential and conserved host-colonization factor. *P Natl Acad Sci USA.* 2011;108(27):11217-22
38. Xu Q, Christen B, Chiu HJ, Jaroszewski L, Klock HE, Knuth MW, et al. Structure of the pilus assembly protein TadZ from *Eubacterium rectale*: implications for polar localization. *Mol. Microbiol.* 2012;83(4):712-27.
39. Ventura M, Turroni F, Motherway MO, Macsharry J, Sinderen D. Host-microbe interactions that facilitate gut colonization by commensal bifidobacteria. *Trends Microbiol.* 2012;20(10):467-76.
40. Paone P, Cani PD. Mucus barrier, mucins and gut microbiota: The expected slimy partners? *Gut.* 2020;69(12):2232-43.
41. Langmead B, Salzberg SL. Fast gapped-read alignment with Bowtie 2. *Nat Methods.* 2012;9(4):357-9.
42. Anders S, Pyl PT, Huber W. HTSeq—a Python framework to work with high-throughput sequencing data. *Bioinformatics.* 2015;(2):166-9.
43. Anders S. Analysing RNA-Seq data with the DESeq package. *Mol. Biol.* 2010;43:1-17.
44. Xiong Y, Zhai Z, Lei Y, Xiao B, Hao Y. A novel major pilin subunit protein FimM is involved in adhesion of *Bifidobacterium longum* BBMN68 to intestinal epithelial cells. *Front. Microbiol.* 2020;11:590435.

## Figures

### Figure 1

Growth of *B. lactis* A6 strain in MRSc broth incubated at 37°C for 24 h. The OD600 and pH were changed with time from 0 to 24 h; *B. lactis* A6 grew up to an average OD600 around 0.6~0.8 was collected as the exponential phase samples (n=4, T0), while OD600 around 4.0~4.2 was collected as the stationary phase samples (n=3, T1).

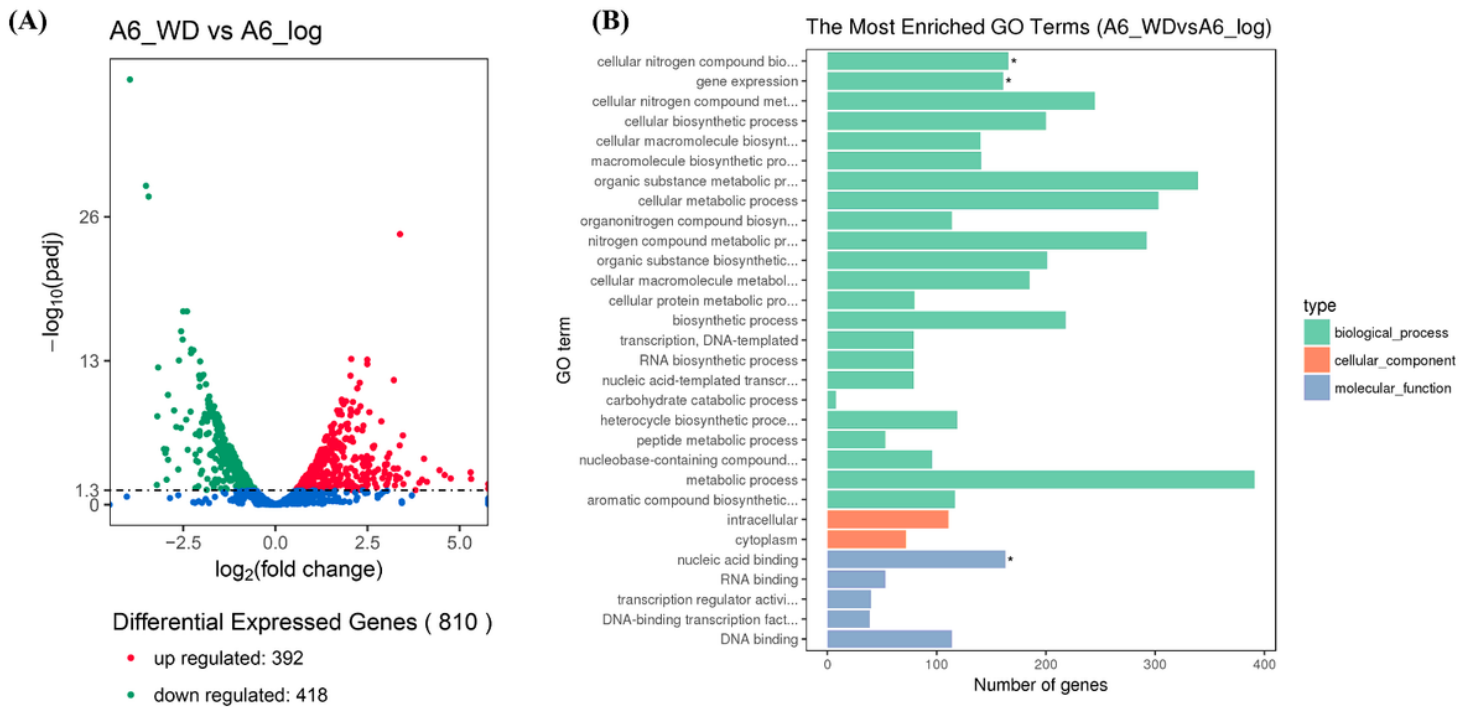


**Figure 2**

RNA-seq analysis of differentially expressed genes. (A) Volcano plot of DEGs during the stationary phase (A6\_WD) compared to the log phase (A6\_log). The red plots represent upregulated genes, and the green plots represent downregulated genes. (B) Distribution of DEGs during A6\_WD compared to A6\_log. The length of each bar indicates the gene numbers involved in certain GO term. Asterisk (\*) indicates significantly enriched GO terms.

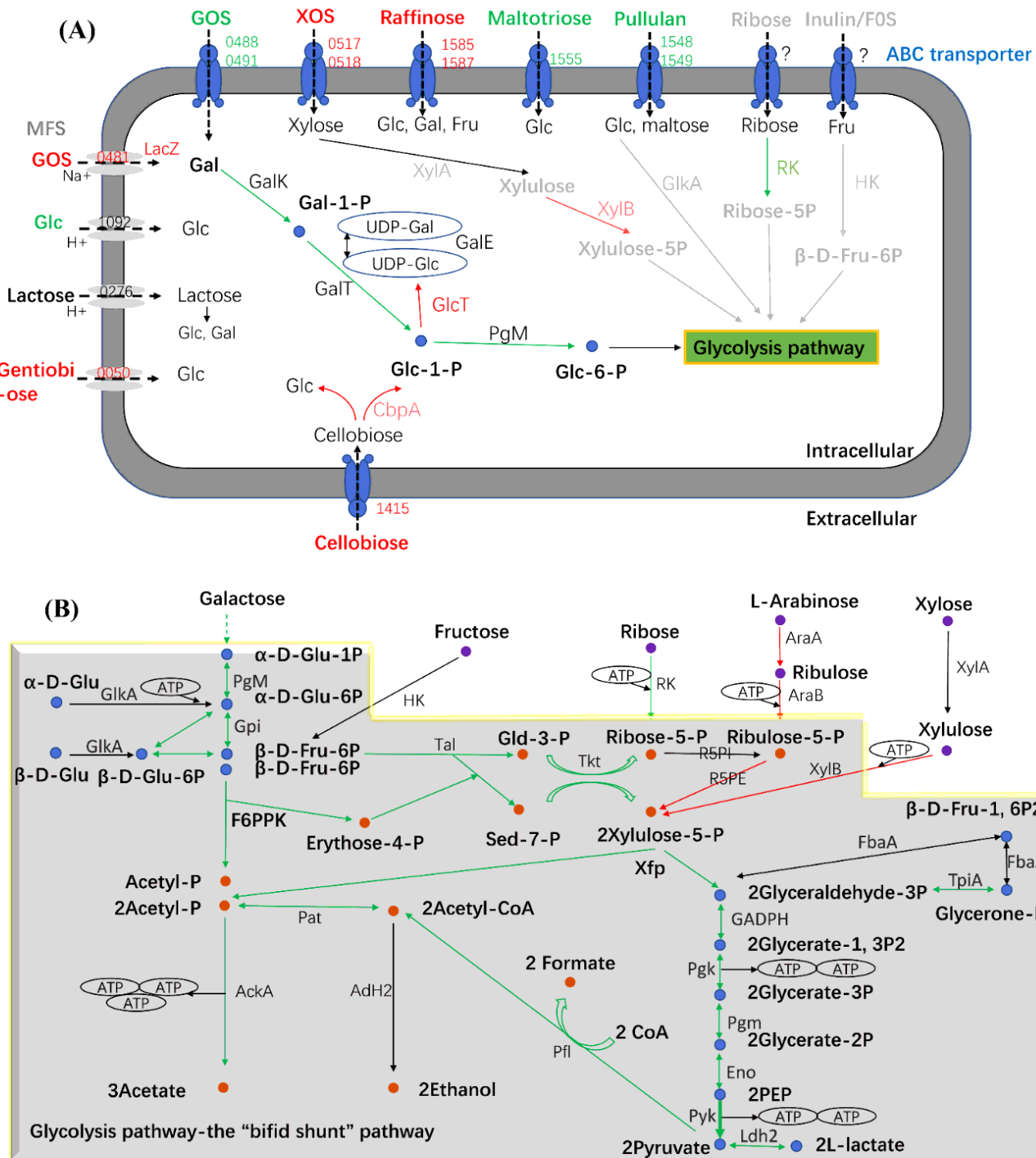


**Figure 3**

Graphical representation of genes involved in carbohydrates transport (A) and metabolism (B) of *B. animalis* subsp. *lactis* A6 in the stationary phase compared to the log phase. GOS, galactooligosaccharides; XOS, xylooligosaccharides; FOS, fructooligosaccharides; Gal-1-P, galactose-1-phosphate; Glc-1-P, glucose-1-phosphate; Glc-6-P, glucose-6-phosphate; β-D-Fru-6P, β-D-fructose-6-phosphate; UDP-Gal, uridine diphosphate galactose; UDP-Glc, Uridine diphosphate glucose; Gld-3-P,



glyceraldehyde 3-phosphate; Sed-7-P, sedoheptulose 7-phosphate; GalK, galactose kinase; GalT, galactose-1-phosphate uridylyltransferase; GalE, UDP-glucose 4-epimerase; GlcT, glucosyltransferase; CbpA, cellobiose phosphorylase; XylA, xylose isomerase; XylB, xylulokinase; GlkA, glucokinase; PgM, phosphoglucomutase; Gpi, glucose-6-phosphate isomerase; F6PPK/Xfp, fructose-6-phosphate/Xylulose-5-phosphate phosphoketolase; FbaA, fructose-bisphosphate aldolase; TpiA, triosephosphate isomerase; GADPH, glyceraldehyde 3-phosphate dehydrogenase; Pkg, phosphoglycerate kinase; Pgm, phosphoglyceromutase; Eno, enolase; Pyk, pyruvate kinase; Ldh2, lactate dehydrogenase; Pfl, formate acetyltransferase; Pat, phosphate acetyltransferase; AckA, acetate kinase; Adh2, bifunctional acetaldehyde-CoA/alcohol dehydrogenase; Tal, transaldolase; Tkt, transketolase; RK, ribose kinase; R5PI, ribose-5-phosphate isomerase; R5PE, ribulose-phosphate 3-epimerase; PEP, phosphoenolpyruvate. Arrows or gene numbers in black, red or green color show genes which are unchanged, up-regulated or down-regulated at transcriptional level, respectively.

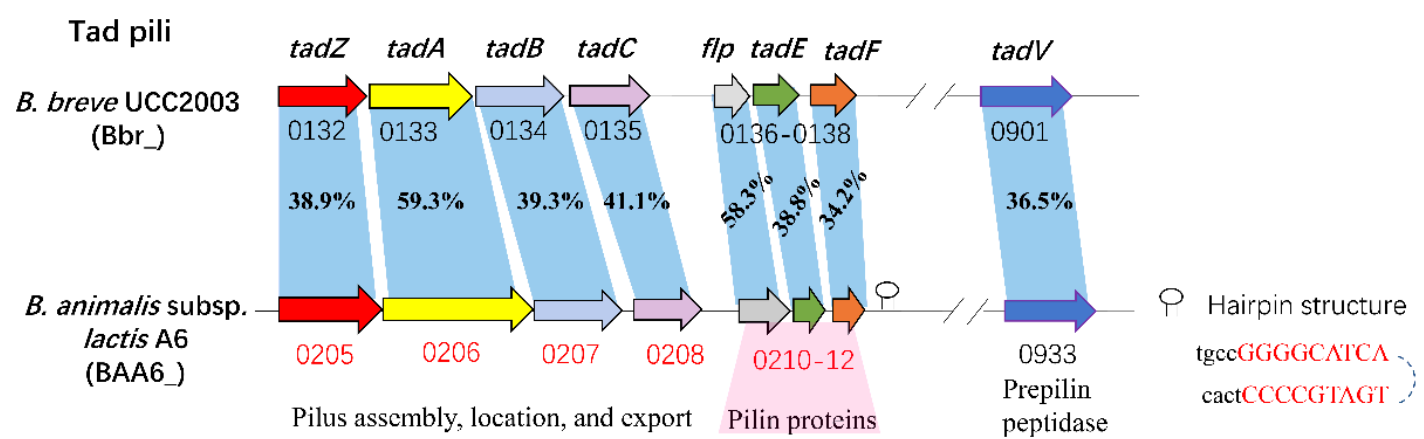


**Figure 4**

Schematic representation of the tad locus involved in pilus biosynthesis of *B. lactis* A6 compared with *B. breve* UCC2003. Each arrow represents an open reading frame (ORF), and the size of which is proportional to the length of the arrow. Gene name or gene number is right above or below the arrow. Coloring of the arrows represents the different function of the gene as indicated above each arrow. For *B. lactis* A6, gene numbers in red or black indicate transcriptionally up-regulated or unchanged genes during the stationary phase compared to the log phase. The amino acid identity of the relevant encoded proteins is indicated in percentages. A predicted transcription terminator with a hairpin structure is indicated by the stem loop.

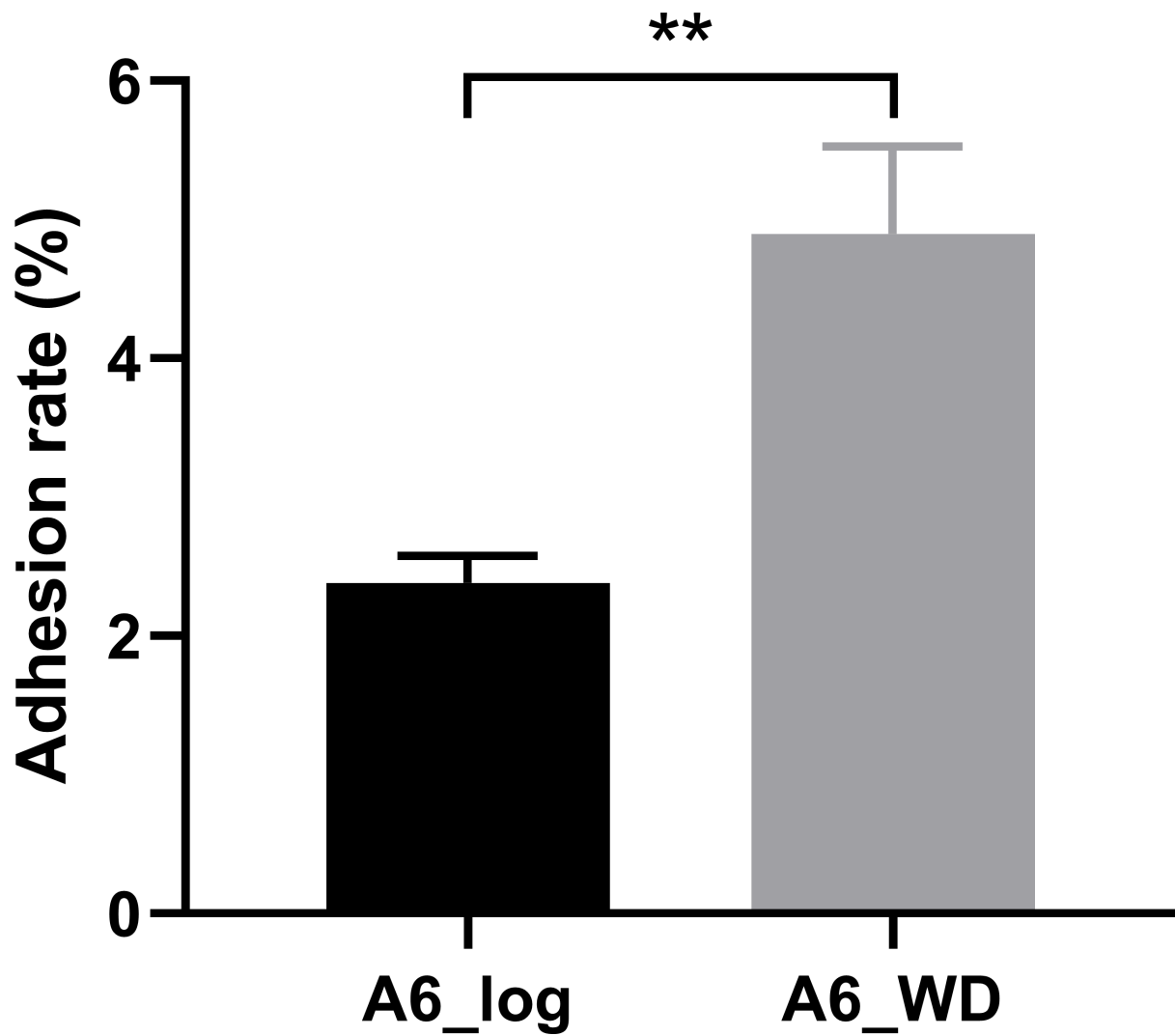


**Figure 5**

Adhesion rate to mucin. Statistically significant differences between the exponential phase (A6\_log) and the stationary phase (A6\_WD) were identified using an unpaired student t-test. (n=3; \*\*, p < 0.01).

## Supplementary Files

This is a list of supplementary files associated with this preprint. Click to download.

- [Supplementalmaterials.docx](#)